

SPATIAL DISTRIBUTION OF STABLE WATER-ICE CONSIDERING ENGINEERING CONSTRAINTS IN THE LUNAR SOUTH POLAR REGION. C. Orgel¹, E. Sefton-Nash¹, T. Warren², S. J. Boazman¹, O. King², N. Bowles². ¹European Space Research and Technology Centre (ESTEC), European Space Agency, Noordwijk, NL (csilla.orgel@esa.int), ²Dept. of Atmospheric, Oceanic and Planetary Physics, University of Oxford, UK.

Landing site assessment: The South Pole of the Moon and its potential for cold-trapped volatiles to persist [1, 2, 3, 4, 5] became the focus for future landed missions. Landing site selection for any surface mission typically involves optimizing a balance between quantities or criteria that indicate the extent to which the mission's objectives can be met or exceeded. Oftentimes, a first step is to filter out unviable landing sites by applying operational or engineering requirements to environmental or terrain characteristics, and a second step amounts to optimization or trade-off to maximize satisfaction of mission objectives, including potential science return [6].

In this study we show results quantifying the probability of being able to target areas where thermal conditions permit the long-term stability of cold-trapped volatiles in the shallow sub-surface. Leading thermophysical model results [2, 7] indicate zones of thermal stability are preferentially distributed in the top few 10s of cm. We also consider factors related to mission operations, namely: Earth visibility for direct-to-Earth communication and solar illumination for power.

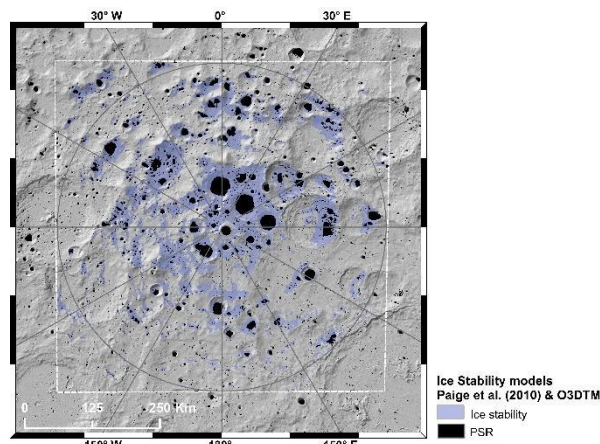


Figure 1: Areas in which volatile stability is predicted both by data from [2] and [7]. Note that intersection is only possible in areas of mutual coverage, within the bounding box of data from [2]. PSRs [8] are shaded black.

Data and Methods: We combine datasets sampled at a spatial resolution of 120 m/pix, spatial coverage extending from the pole to 80°S at the cardinal meridians, and including metrics of volatile stability [2, 7] as indicators of science potential (Figure 1), as well as LOLA derived slope [9], average solar

illumination, and Earth visibility [8] maps following the work from [6]. We prepared boolean rasters that are true where terrain is compliant with scientific and engineering constraints in Table 1. We used the Conditional Tool in ArcGIS 10.7 software and MATLAB to derive the maps and histograms.

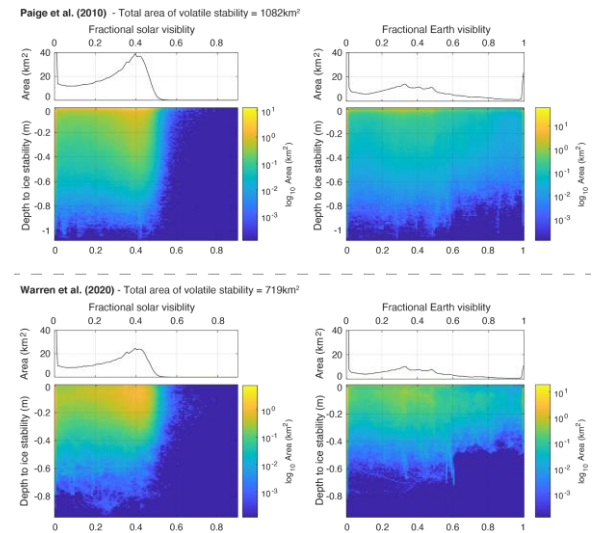


Figure 2: Distribution of depth to water ice stability data from (upper panels) [2] and (lower panels) [7] with respect to (left panels) mean fractional solar visibility, and (right panels) mean fractional Earth visibility [8]. Line plots are histograms of the total area covered in each bin. Color plots are 2D histograms of \log_{10} of the area in km^2 . Bin sizes are 0.01 in meters (depth to ice stability) and 0.01 in mean fractional visibility.

Distribution of depth to water ice stability: We plot the distribution of depth to water ice stability data from both thermophysical models [2, 7] compared with the mean fractional solar visibility and Earth visibility (Figure 2). Within the same study area, thermal model results indicate a total area in which water ice is stable of 1082 km^2 [2] and 719 km^2 [7], respectively.

Scenarios: We define two scenarios, one more constrained, and one less constrained, to explore the distribution of compliant terrain, both spatially and in selected parameter spaces of the constraining criteria. Thresholds in slope, solar illumination, and Earth visibility (Table 1) were selected regarding the general case of a solar powered lunar polar lander using direct-to-Earth communications.

Figure 3 illustrates the spatial distribution of compliant terrain for the least and most constrained cases, but

without applying the boolean mask of volatile stability (Figure 1), i.e. the first three rows in Table 1. Figure 4 represents the effect of further constraint of the mask in Figure 3 to only locations where volatile stability is also indicated by both thermal models [2, 7]. Adding the scientific constraint to the engineering constraints significantly decreases the areal coverage of suitable landing sites.

Dataset	Least constrained scenario	Most constrained scenario
LOLA derived slope, °	$\leq 15^\circ$	$\leq 7^\circ$
Earth visibility (%)	25%	50%
Solar illumination (%)	15%	35%
Volatile stability	True	True

Table 1: Scenarios defined by thresholds on datasets.

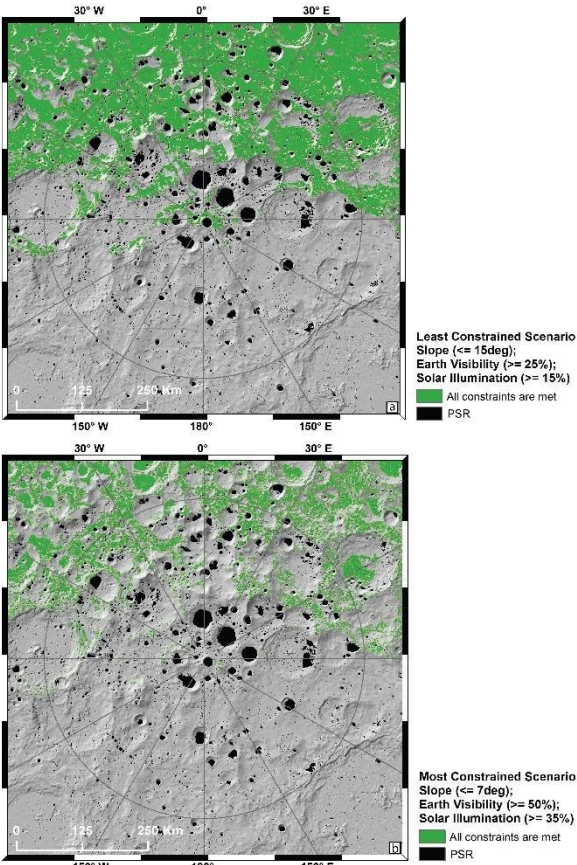


Figure 3: Mask of terrain with compliant slope, Earth visibility, and solar illumination. (A) Least constrained scenario with slope $\leq 15^\circ$, Earth visibility $\geq 25\%$, and solar illumination $\geq 15\%$ layers. (B) Most constrained scenario with slope $\leq 7^\circ$, Earth visibility $\geq 50\%$, and solar illumination $\geq 35\%$ layers.

Future work: We aim to investigate the likelihood of landing in a preferable location based on the landing precision of a landing system [10].

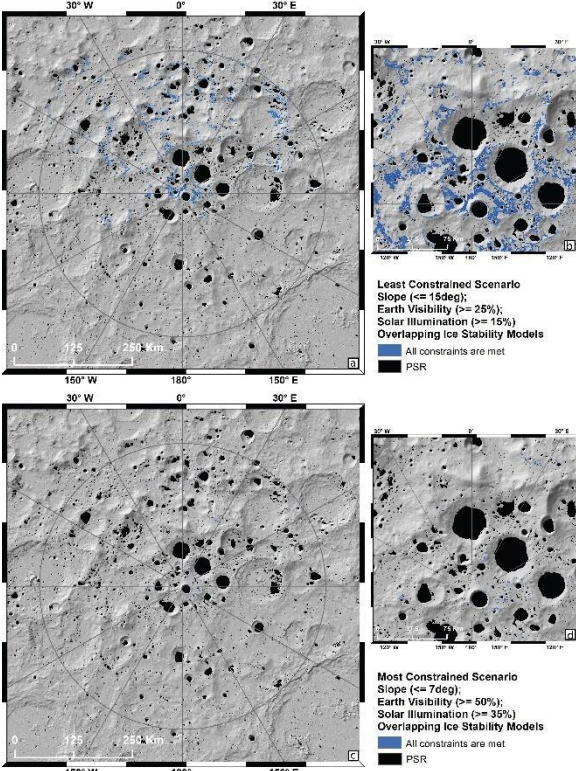


Figure 4: Mask of terrain with compliant slope, Earth visibility, solar illumination and ice stability criteria. Note that data are implicitly cropped to the spatial extent of where ice stability is predicted by models of both [2] and [7]. (A) Least constrained scenario with slope $\leq 15^\circ$, Earth visibility $\geq 25\%$, solar illumination $\geq 15\%$, and overlapping ice stability layers. (B) Image subset of the spatial distribution of suitable locations around the South Pole for the least constrained scenario. (C) Most constrained scenario with slope $\leq 7^\circ$, Earth visibility $\geq 50\%$, and solar illumination $\geq 35\%$ and overlapping ice stability layers [2, 7]. (D) Zoomed view of the spatial distribution of suitable locations around the South Pole for the most constrained scenario.

References: [1] Ingersoll, A. P.T. et al., (1992). Icarus 100, 40–47. [2] Paige, D. A. et al., (2010). Science 330(6003): 479. [3] Hayne, P.O. et al. (2015). Icarus 255, 58–69. [4] Hayne, P.O. et al. (2020). Nature Astronomy 5, 169–175. [5] Flahaut, J. et al., (2020). Planetary and Space Science 180: 104750. [6] Djachkova, M V et al. (2017). Solar System Research 51(3): 185–95. [7] Warren, T. et al., (2020). <https://github.com/tw7044/O3DTM/>. [8] Mazarico, E. et al., (2011). Icarus 211(2): 1066–81. [9] Smith, D. E. et al., (2017). Icarus, 283, 70–91. [10] Boazman, S. J. et al. (2022), LPSC, this conf.